Size-Dependent Evolution of Graphene Nanopores Under Thermal Excitation

*Tao Xu, Kuibo Yin, Xiao Xie, Longbing He, Binjie Wang, and Litao Sun**

Nanopores embedded in thin membranes have attracted global attention because of their potential application in label-free, single-molecule detection of chemicals or biomolecules.[1–4] A nanopore of 1–5 nm exhibits a distinct size effect, making it particularly suitable for characterizing most biomolecules. For example, protein nanopores[5,6] and solid-state nanopores (embedded in silicon nitride,[7,8] silicon oxide,[9] or aluminum oxide[10–12] membranes) have been used to detect single-strand DNA or RNA. Although solid-state nanopores exhibit high stability, the thickness of membranes are typically large with low resolution along the pore axis which can't be used to obtain precision information on biomolecules (e.g., sequence of base pairs in DNA). Thus, nanopores based on graphene material have been applied as alternative solutions to this problem. Aside from the exceptional mechanical properties of few-layer graphene, its thickness (~0.34 nm per layer) well corresponds with the distance between adjacent base pairs on stretched DNA (~0.36 nm), thereby enabling graphene nanopores to access single-base resolution on DNA.[13–15] However, conventional nanofabrication techniques constrain the precise modulation of pore morphology. Drilling nanoscale pores by focused electron beam-induced processing inside a transmission electron microscope (TEM) enables the effective fabrication of nanopores with defined diameters because of the sputtering effect[16–20]. However, this technique is not fully controllable at nanoscale because real-time imaging cannot be synchronously performed with drilling, which leads to morphological defects in nanopores.

To fabricate small nanopores with fine pore morphology, researchers modulate the morphology of as-fabricated nanopores by electron beam irradiation at optimized electron intensity.[16,17] Given the electron beam-induced surface tension, the atoms can be activated to form a mass flow, which can reconstruct nanopore edges, thereby modifying nanopore geometry. Nevertheless, electron irradiation can damage the crystalline structure of the membrane, causing amorphism, especially in materials with low displacement energy; an example of such materials is carbon,[20] whose atom displacement energy is 15–20 eV (out of plane) and 30 eV (in-plane) for graphite.[21] These atom displacement energies mean that electrons carry energies greater than 100 and 140 keV, respectively. Therefore, the structure or morphology of fabricated nanopores becomes unstable, which may increase the fragility of and noise in nanopore-based nanodevices, as well as limit their application in DNA sequencing and single-molecule analysis. According to previous studies, radiation damage can be avoided or minimized by the heat effect because heat treatments, or thermal annealing, may promote the self-repair of the crystallinity of carbon materials, including graphene.[19,22]

In this paper, we modulate the morphology of graphene nanopores by in situ thermal heating on a TEM. Direct thermal heating on this instrument can avoid the absorption of contaminants and help fine-tune nanopore size and crystallinity. Our results show that the size of the fabricated nanopores can be precisely reduced or enlarged, depending on the relationship between the diameter of the nanopore and the thickness of graphene membrane. As we will show in this paper, the thermal-induced migration of uncombined carbon atoms energetically prefer to form a stable structure with low free surface energy.

Figure 1a shows that the nanopores were fabricated on the graphene membranes by a highly focused electron beam. During nanopore fabrication, the electron beam was carefully adjusted and quickly moved to a fresh region on the graphene sheet at a pre-defined irradiation time less than 20 s. When the fabrication process was complete, the electron beam was quickly sheltered and then widely distributed to minimize irradiation damage during routine imaging. The nanopore temperature was maintained at above 400 °C for at least 30 min without irradiation. Finally, the nanopores with sizes comparable to those of the as-fabricated nanopores were imaged by a spread electron beam to determine whether shrinkage or expansion has occurred. Figure 1b–c show the typical shrinkage of graphene nanopores with an initial diameter of ~3.8 nm at 400 °C, while Figure 1d–e show the expansion of nanopores with an initial diameter of ~7.8 nm at 400 °C.

Figure 2a–c demonstrate the typical shrinkage of graphene nanopores under thermal heating. The nanopores

T. Xu, Dr. K. Yin, Dr. X. Xie, Dr. L. He, Dr. B. Wang, Prof. L. Sun
SEU-FEI Nano-Pico Center
Key Lab of MEMS of Ministry of Education
Southeast University
Nanjing, 210096, PR China
E-mail: slt@seu.edu.cn
Dr. B. Wang
FEI Company
Shanghai Nanoport, No. 690 Bibo Road, Shanghai, 201203, PR China

DOI: 10.1002/smll.201200979

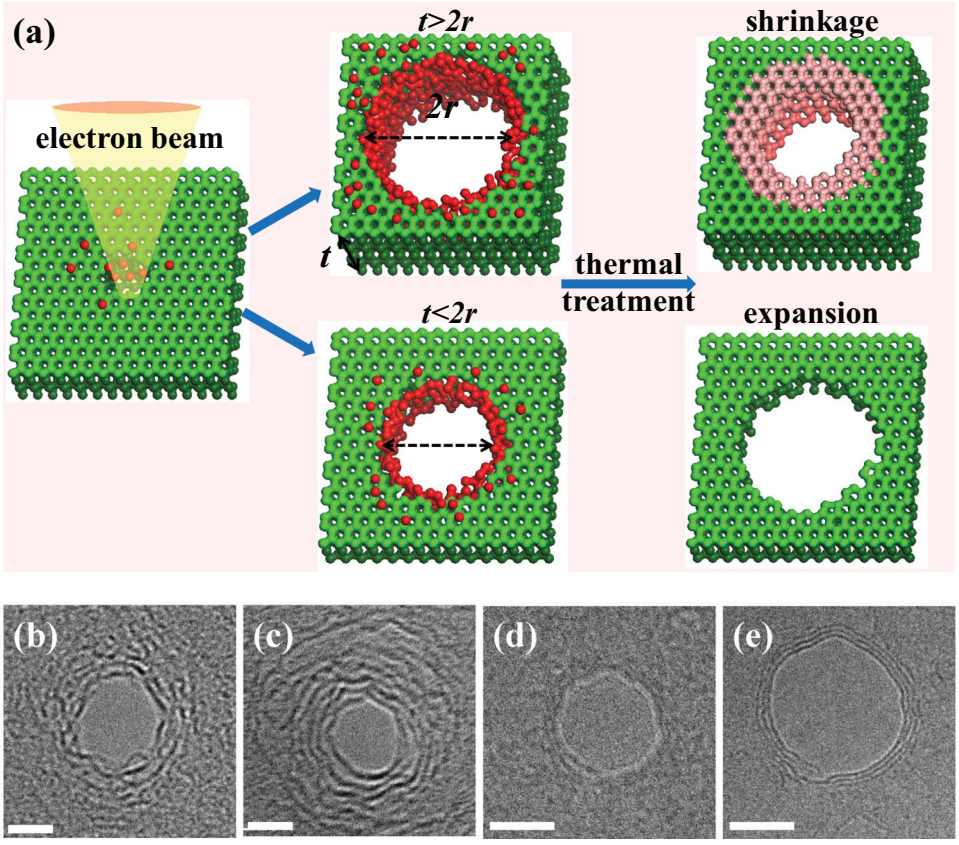

Figure 1. TEM image of the fabrication and evolution processes of graphene nanopores: (a) Schematic of the experiment illustrating the fabrication and evolution processes of graphene nanopores and (b–e) TEM images showing nanopore shrinkage (b–c) or expansion (d–e) under thermal excitation. The scale bar is 2 nm in (b–c) and 5 nm in (d–e).

with an initial mean diameter ($2\sqrt{S/\pi}$, where S is the area of the nanopores) of 4.2 nm were drilled at room temperature (RT) by a converged electron beam for 20 s (Figure 2a). The thickness of the graphene membrane was estimated at ~6 nm because the dark rim of the nanopores represent connected adjacent graphene layers or back folding.[23,24] The graphene around the pores becomes amorphous due to electron irradiation. Then, 55 min after the temperature has been increased to 450 °C without irradiation, the average diameter of the nanopores decreases from 4.2 to 3.3 nm (Figure 2b), and the edge of the nanopores appears very different from that before heat treatment. Before thermal treatment, amorphization is observed, leading the edge of the pore unclear. However, after being heated, a clear terrace-like structure can be seen around the as-fabricated nanopores. Another 13 min later, the pore diameter slightly changes and then stabilizes at 3.2 nm, and the edge of the terrace-like structure becomes clearer. The evolution of pore edge indicates that thermal effect may not only change the sizes of nanopores but also recrystallize amorphous carbon, which is attributed to the saturation of dangling bonds and the migration of defects at temperature higher than 300 °C.[22] Interestingly, the graphene nanopores drilled at 400 °C also shrink as a function of time at the same temperature, although the change in diameter is minimal. More examples on shrinkage of nanopores with various diameters and thicknesses under thermal excitation are given in Figure S1.

Nanopores can also tend to expand under electron irradiation. In this study, we visibly observed the expansion of nanopores under thermal heating without irradiation. Figure 2d–f shows the expansion of a 5.6 nm nanopore in a ~5.1 nm thick graphene membrane, which was also drilled at RT. Then, the temperature was raised to 450 °C. After 40 min, the nanopore diameter expands from 5.6 to 7.0 nm at 450 °C, as shown in Figure 2e. However, the diameter of the nanopores changes little after another 20 min of heating, before eventually stabilizing at 6.9 nm. Other typical expansions of nanopores are also given in Figure S2.

The thermal effect can cause the shrinkage and expansion of graphene nanopores. To investigate the mechanism of the thermal effect on nanopore size, we repeated nanopore fabrication with thermal-assisted modulation. A total of 70 nanopores were investigated and the results are shown in **Figure 3**. The findings confirm the shrinkage and expansion effect of heat treatment. Specifically, 26 nanopores expand and the remaining 44 shrink. Meanwhile, 40 (97.6%) out of 41 nanopores, with initial pore diameters smaller than membrane thicknesses, shrink after heat treatment, whereas 25 (86.2%) out of 29 nanopores, with initial diameters greater than membrane thicknesses, expand. Some nanopores slightly

small 2012,
DOI: 10.1002/smll.201200979

small NANO MICRO

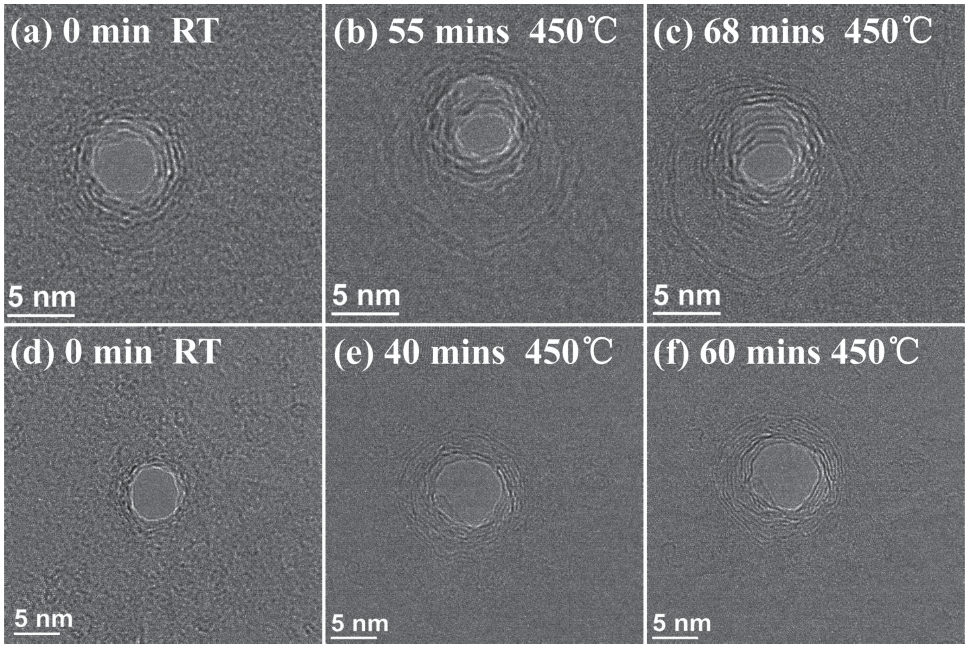

Figure 2. Evolution processes of graphene nanopores: (a) Nanopores drilled at RT with initial diameters of ~4.2 nm and (b–c) nanopores of (a) after being heated at 450 °C for 55 and 68 min. The mean diameter of the pores decreases to 3.3 nm and then stabilizes at 3.2 nm. (d) Nanopores drilled at RT with an initial diameter of ~5.6 and (e–f) nanopores of (d) after being heated at 450 °C for 40 and 60 min. The mean diameter of the pores expands to 7.0 nm and then stabilizes at 6.9 nm.

deviate from the law shown in Figure 3, which could be due to the errors in thickness estimation. Because the graphene thickness cannot be directly measured from TEM images, calculating the graphene layers around the inner fringe of the nanopores may induce inevitable uncertainty. However, statistical study of nanopores with diverse diameters versus graphene thicknesses intuitively exhibited the dominant regime of the nanopore evolutions. In Figure 3, the dashed line (which indicates the initial nanopore diameter equal to the membrane thickness) denotes the criterion for pore shrinkage and expansion. The change in the size of graphene nanopores (increasing or decreasing) depends on the ratio of initial pore diameter to membrane thickness.

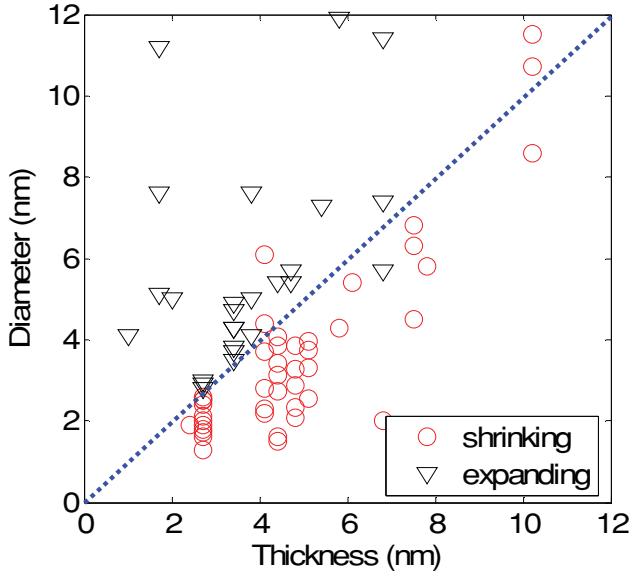

Figure 3. Data on the shrinking or expanding pores with different initial diameters and thicknesses. The red circles on the diagram represent shrinkage under direct thermal heating, whereas the black triangles represent expansion. The blue dotted line illustrates the case when pore diameter is equal to pore thickness.

The physical shrinkage or expansion mechanism of graphene nanopores can be explained by the thermal-induced migration of uncombined carbon atoms, which energetically prefer to form a stable structure with low free surface energy. The amount of carbon adatoms determines the extent of diameter change.

The carbon atoms knocked out by electrons and hydrocarbons adsorbed on samples are the main sources of carbon adatoms. Regardless of their origin, carbon adatoms are highly mobile at temperatures above 300 °C.[21] Hence, the adatoms at high temperature can diffuse to low free surface energy F of the system. If the graphene nanopore structure is simplified as cylindrical with radius r embedded in the graphene membrane with constant thickness t, we can calculate the change in free energy in relation to an intact sheet using the following equation:[16]

$$\Delta F = \gamma \Delta A = 2\pi\gamma \left(rt - r^2\right) \quad (1)$$

Where γ is the surface tension of the mobile interstitial carbon atoms and ΔA denotes the change in surface area. Under such an assumption, free surface energy decreases with the expansion of nanopores when r > t/2, or with the shrinkage of nanopores when $r < t/2$. This result agrees with

DOI: 10.1002/smll.201200979

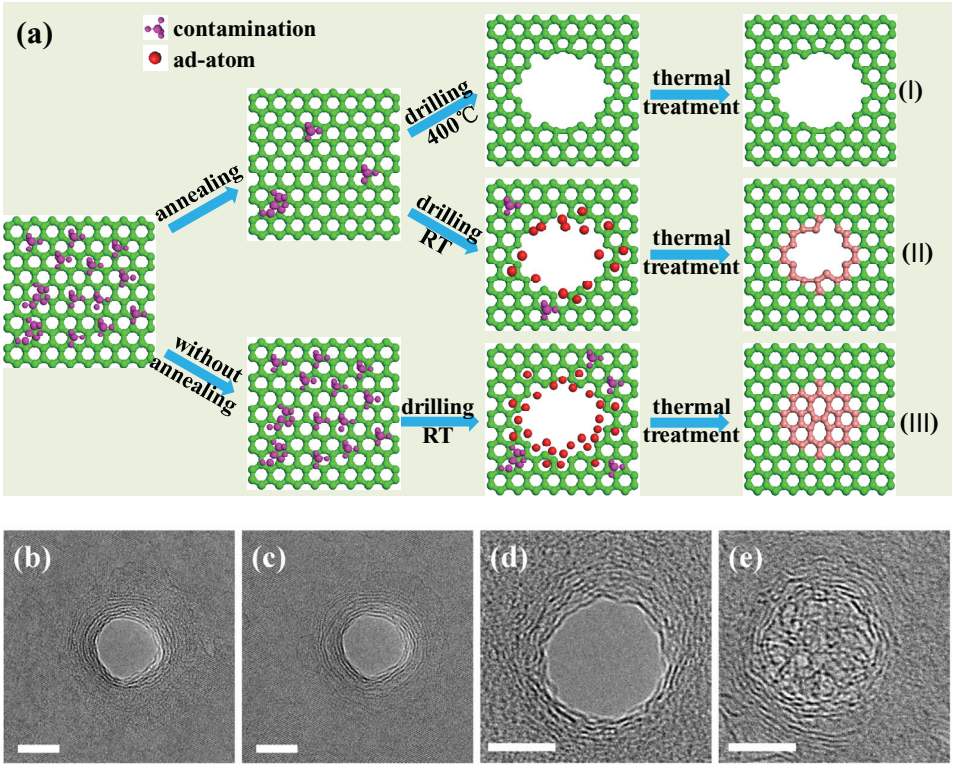

Figure 4. Different amounts of carbon adatoms in the evolution of graphene nanopores: (a) Schematic of the evolution of graphene nanopores under different conditions. (b–e) TEM images of the evolution of nanopores drilled at 400 °C (b–c) and nanopores drilled at RT without annealing (d–e) under thermal excitation. The nanopores drilled at 400 °C with an initial diameter of ~7.0 nm slightly changes in size, whereas the nanopores drilled at RT close after being heated at 450 °C for 90 min. The scale bar in (b–e) is 5 nm.

the experimental findings (Figure 3). During heat treatment, ΔF always decreases, indicating that of the change in nanopore size is mediated primarily by the free surface energy.

Lastly, the relationship between the amount of carbon adatoms and the evolution of pore sizes has been discussed. Two main sources of carbon adatoms were used in the experimental system: the interstitial atoms generated by the irradiation effect and the adatoms produced by the decomposition of the adsorbed hydrocarbons. Electrons with energies greater than 100 keV[21] damage the graphene crystal structure at RT, generating undesired interstitial atoms. A large amount of knocked out carbon atoms exist in the area exposed to the electron beam. At the same time, nanopore area is always smaller than beam size. Therefore, a damaged region always exists around the inner fringe of a nanopore, which contains many uncombined carbon atoms. Hydrocarbon contamination, on the other hand, is induced and decomposed onto the sample by the electron beam, which also considerably affects the change in nanopore size.

As shown in **Figure 4**a, substantial contamination is desorbed under pre-annealing before the nanopores were fabricated under conditions I and II. In these cases, minimal contamination is absorbed on the graphene membrane. The adatoms mainly originate from the knocked out atoms in the damaged region during high-dose irradiation in the drilling process. The difference was that the nanopores were drilled at 400 °C and RT under conditions I and II, respectively. During the drilling process at 400 °C, some knocked out carbon atoms diffuse and form a stable structure through dangling bond saturation. Hence, fewer adatoms are produced, causing obscure change in nanopore diameter under condition I. Without pre-treatment, substantial contamination is observed in the samples treated under condition III; the contamination supplied an additional carbon source under electron radiation. The change observed under condition III is more visibly observable under thermal treatment. Figure 4b–c shows the TEM images of the nanopores drilled at 400 °C; these nanopores exhibit little change under the same temperature. By maintaining this temperature for 60 min without irradiation, the diameter of the pore decreases only by 0.1 nm (i.e., from 7.0 to 6.9 nm). The same situation occurs with the subtle changes in Figures 2b–c and e–f. Figure 4d–e present completely closed nanopores at 450 °C. The nanopores were drilled at RT without any heat pre-treatment for contamination cleaning. Thus, considerable carbon contamination is adsorbed onto the graphene membrane, thereby producing numerous adatoms under electron radiation. After being annealed for 90 min, the nanopores completely close. The structure of the filled region differs from the other areas in the membrane, as shown in Figure 4e. The control experiment in Figure 4 confirms that the amount of adatoms determines the extent of diameter change, and that contamination is a major source of adatoms.

In conclusion, graphene nanopores can shrink or expand by direct thermal heating dependent on the ratio of nanopore diameter to membrane thickness. At the same time, the extent

small 2012,
DOI: 10.1002/smll.201200979

NANO MICRO small

of diameter change depends on the quantity of uncombined atoms, and the amorphous area around the hole recrystallize under thermal annealing. Such a size-dependent evolutionary mechanisms of nanopores considered as thermal-induced migration of uncombined carbon atoms, which also proved by exprements. The in situ TEM fabrication technique combined with direct thermal heating serves as an effective strategy for fabricating graphene nanostructures of high crystallinity. Such nanostructures present promising potential for chemical and biological applications in which graphene nanodevices are used.

Experimental Section

Graphene was prepared by exfoliating expanded graphite using high-powered ultrasonication,[25] then it was transferred onto a hole in the carbon-coated TEM copper grid. The thickness of the graphene sheets was determined by imaging a folded edge of the nanopores,[19,20] which mostly ranges from 2 to 25 layers (0.7–8.5 nm). Nanopores were drilled on the pristine graphene sheets in an image aberration-corrected TEM (FEI Titan 80–300 at 300 kV) equipped with a heating sample holder (GatanTM 628). To remove the contamination induced by adsorbed hydrocarbon molecules, we maintained the specimen temperature above 300 °C for 30 min before further processing.[26] The nanopores were fabricated on the graphene membranes by a highly focused electron beam (5–10 nm spot diameter, current density ~10^8 electrons nm^{-2}) under a magnification of 550 k×. During nanopore fabrication, the electron beam was carefully adjusted and quickly moved to a fresh region on the graphene sheet at a pre-defined irradiation time less than 20 s. When the fabrication process was complete, the electron beam was quickly sheltered and then widely distributed to minimize irradiation damage during routine imaging, at which the current density is lower than 10^6 electrons nm^{-2}.

Supporting Information

Supporting Information is available from the Wiley Online Library or from the author.

Acknowledgements

This work was supported by the National Basic Research Program of China (Grant Nos. 2011CB707601 and 2009CB623702), the National Natural Science Foundation of China (Nos. 51071044, 60976003, 61006011 and 61106055), Specialized Research Fund for the Doctoral Program of Higher Education (Nos. 20100092120021 and 20100092110014) Program for New Century Excellent Talents in University (No. NCEF-09-0293) and Open Research Fund of State Key Laboratory of Bioelectronics.

[1] S. Howorka, Z. Siwy, *Chem. Soc. Rev.* **2009**, *38*, 2360.
[2] C. Dekker, *Nat. Nanotechnol.* **2007**, *2*, 209.
[3] B. M. Venkatesan, R. Bashir, *Nat. Nanotechnol.* **2011**, *6*, 615.
[4] L. Gu, J. W. Shim, *Analyst.* **2010**, *135*, 441.
[5] F. Olasagasti, K. R. Lieberman, S. Benner, G. M. Cherf, J. M. Dahl, D. W. Deamer, M. Akeson, *Nat. Nanotechnol.* **2010**, *5*, 798.
[6] J. J. Kasianowicz, E. Brandin, D. Branton, D. W. Deamer, *Proc. Natl. Acad. Sci. USA* **1996**, *93*, 13770.
[7] J. Li, M. Gershow, D. Stein, E. Brandin, J. A. Golovchenko, *Nat. Mater.* **2003**, *2*, 611.
[8] M. Wanunu, T. Dadosh, V. Ray, J. Jin, L. McReynolds, M. Drndic, *Nat. Nanotechnol.* **2010**, *5*, 807.
[9] H. Chang, F. Kosari, G. Andreadakis, M. A. Alam, G. Vasmatzis, R. Bashir, *Nano Lett.* **2004**, *4*, 1551.
[10] B. M. Venkatesan, A. B. Shah, J.-M. Zuo, R. Bashir, *Adv. Funct. Mater.* **2010**, *20*, 1266.
[11] B. M. Venkatesan, B. Dorvel, S. Yemenicioglu, N. Watkins, I. Petrov, R. Bashir, *Adv. Mater.* **2009**, *21*, 2771.
[12] B. M. Venkatesan, D. Estrada, S. Banerjee, X. Jin, V. E. Dorgan, M.-H. Bae, N. R. Aluru, E. Pop, R. Bashir, *ACS Nano* **2011**, *6*, 441.
[13] S. Garaj, W. Hubbard, A. Reina, J. Kong, D. Branton, J. A. Golovchenko, *Nature* **2010**, *467*, 190.
[14] C. A. Merchant, K. Healy, M. Wanunu, V. Ray, N. Peterman, J. Bartel, M. D. Fischbein, K. Venta, Z. T. Luo, A. T. C. Johnson, M. Drndic, *Nano Lett.* **2010**, *10*, 2915.
[15] G. F. Schneider, S. W. Kowalczyk, V. E. Calado, G. Pandraud, H. W. Zandbergen, L. M. K. Vandersypen, C. Dekker, *Nano Lett.* **2010**, *10*, 3163.
[16] A. J. Storm, J. H. Chen, X. S. Ling, H. W. Zandbergen, C. Dekker, *Nat. Mater.* **2003**, *2*, 537.
[17] H. Chang, S. M. Iqbal, E. A. Stach, A. H. King, N. J. Zaluzec, R. Bashir, *Appl. Phys. Lett.* **2006**, *88*, 103109.
[18] J. M. Zhang, L. P. You, H. Q. Ye, D. P. Yu, *Nanotechnology* **2007**, *18*, 155303.
[19] B. Song, G. F. Schneider, Q. Xu, G. Pandraud, C. Dekker, H. Zandbergen, *Nano Lett.* **2011**, *11*, 2247.
[20] M. D. Fischbein, M. Drndic, *Appl. Phys. Lett.* **2008**, *93*, 113107.
[21] F. Banhart, *Rep. Prog. Phys.* **1999**, *62*, 1181.
[22] A. V. Krasheninnikov, F. Banhart, *Nat. Mater.* **2007**, *6*, 723.
[23] Z. Liu, K. Suenaga, P. J. F. Harris, S. Iijima, *Phys. Rev. Lett.* **2009**, *102*, 015501.
[24] L. Qi, J. Y. Huang, J. Feng, J. Li, *Carbon* **2010**, *48*, 2354.
[25] K. M. Liao, W. F. Ding, B. Zhao, Z. G. Li, F. Q. Song, Y. Y. Qin, T. S. Chen, J. G. Wan, M. Han, G. H. Wang, J. F. Zhou, *Carbon* **2011**, *49*, 2862.
[26] R. F. Egerton, P. Li, M. Malac, *Micron* **2004**, *35*, 399.

Received: May 6, 2012
Revised: July 20, 2012
Published online: